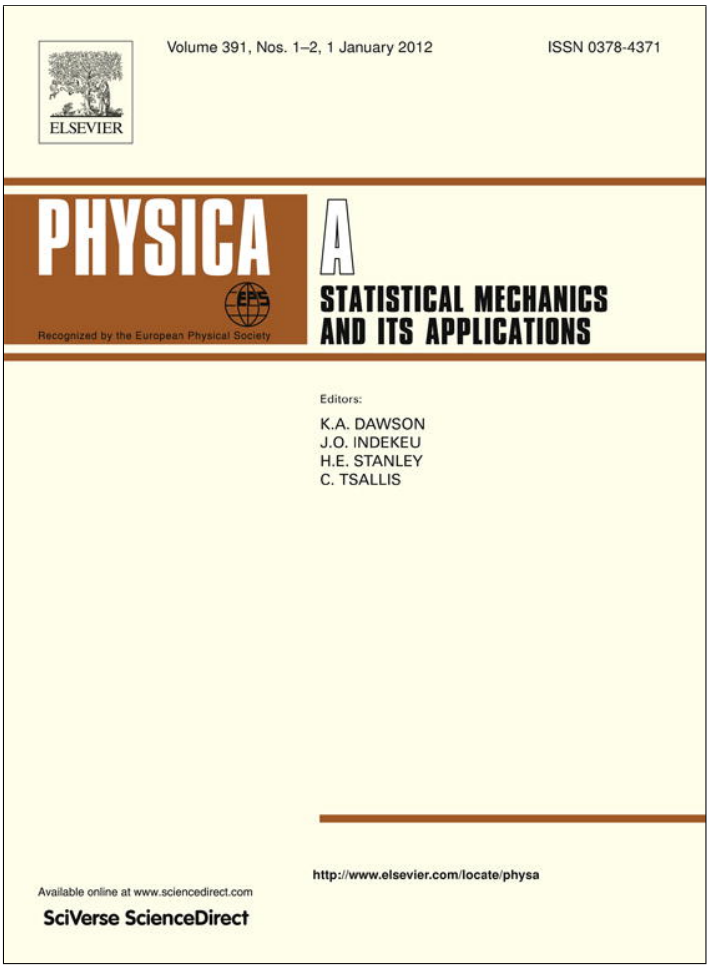

Physica A 391 (2012) 113–124

Contents lists available at SciVerse ScienceDirect

Physica A

journal homepage: www.elsevier.com/locate/physa

A mechanism for pattern formation in dynamic populations by the effect of gregarious instinct

Sergio E. Mangioni [1]

IFIMAR, Instituto de Investigaciones Físicas de Mar del Plata (CONICET–UNMdP), Facultad de Ciencias Exactas y Naturales, Universidad Nacional de Mar del Plata, Deán Funes 3350, (B7602AYL) Mar del Plata, Argentina

ARTICLE INFO

Article history:
Received 28 April 2011
Received in revised form 1 August 2011
Available online 11 August 2011

Keywords:
Aggregation
Pattern formation

ABSTRACT

We introduced the gregarious instinct by means of a novel strategy that considers the average effect of the attractive forces between individuals within a given population. We watched how pattern formation can be explained by the effect of aggregation depending on conditions on food and / or mortality. We propose a model that describes the corresponding dynamic and by a linear stability analysis of homogeneous solutions and can identify and interpret the region of parameters where these patterns are stable. Then we test numerically these preliminary results and find stable patterns as solutions. Finally, we developed a simplified model allowing us to understand in greater detail the processes involved.

1. Introduction

It is known that many species aggregate to form populations of interrelated individuals. The reasons are generally attributed to benefits made when defending against predatory attack and foraging that are superimposed over the corresponding damage by increased competition or disease transmission associated with aggregating [1]. Various structures, seen on a scale that far exceeds the size or even the range of interaction of individual, have surprised more than one observer. For many species dynamics, such as those of some insects, birds, fish, mammals and even crowds of people, these forms can be explained from three simple rules of interaction between individuals: (a) move away from very close neighbors; (b) adopt the same direction as those that are close by and (c) avoid becoming isolated [2]. This (a) implies repulsion, (b) imitation and (c) attraction, effects that are enabled within a certain range of actions. However, the three rules are not equally important in all cases. Sometimes there are more static structures where (b) loses relevance in relation to the other two, being the pattern most affected by the food source than by the movement [3,4]. Conversely, appropriate predictions on how the collective motion (which may be driven by climate change, foraging or defense of a predator) have been made by placing the emphasis on (b) [5]. The models proposed to describe these behaviors are divided into two types: (a) the Lagrangians [6] that focus on individual behavior and Eurelians [7] pointing at a global description. While both strategies can complement each other, the Lagrangians are more appropriate for describing populations of individuals with limited number and relatively large size (birds, fish, mammals, etc.), and the Eurelians, the opposite (microorganisms). In this paper we want to propose a strategy to study the effect of rules (a) and primarily (c) in relation to access to food and mortality. To do this we resort to a mean field model in the framework of reaction diffusion equations with variable diffusion coefficient (Eurelian). This context has been used to model the dynamics of populations of different species [8]. While local interactions between individuals and the environment are described by a nonlinear term, transport is modeled by a diffusion term. Many of these studies have reported successful results in this regard, such as: displaying pattern formation by the effect of local interactions [9]

E-mail address: smangio@mdp.edu.ar.
[1] Member of CONICET, Argentina.

0378-4371/$ – see front matter
doi:10.1016/j.physa.2011.08.001

and non-local [4], both considered in the nonlinear term. In contrast, the explicit effect of aggregation has been considered mainly from Lagrangian models proposing simple rules of interaction similar to those already mentioned and then the collective processes are simulated [6]. Thus, we characterized simultaneously, gregarious effects ordering, access to the food sources and mortality. Our approach can help formalize the link between the above simple rules of individual interaction and the resulting self-organized collective behavior. As already mentioned, by now we focus our attention on rules (a) and (c), leaving (b) for the future. We are not wanting to characterize a particular case, but families of models that attempt to describe patterns in populations of many aggregated individuals, whose sizes are much smaller than the characteristic length of inhomogeneity (for example, microorganisms).

With this expectation, we introduce as a nonlocal effect rules (a) and (c) (these rules may be triggered by senses such as smell, vision, hearing or a chemical process to microorganisms and insects). Unlike Ref. [4]; we incorporate this effect (called by us the gregarious instinct) in the diffusion term, as a result of a current-driven mean field generated by the tendency of individuals to separate (rule a) or join (rule c). To do this we use a strategy similar to the one applied in Refs. [10,11].

Nonlocality of the phenomenon described here is from a different origin to the cases studied previously [4]. In such cases this effect is generally introduced into a term that represents the competition by resources, enhancing it by decreasing the distance between the competitors. In our study, the nonlocal effect, nothing more than the tendency to move away from very close neighbors or congregate them when individuals are widely separated (rules a and c). To clarify this, we visualize the gregarious instinct among individuals from a given population as a force that tends to collect them, when they perceive that they are away from each other and, on the other hand to move away when they are closer to each other.

This kind of force is more effective when individuals are closer together; however, if they are too close it causes the opposite effect. In particular, we investigate possible effects of such an instinct over a population of individuals characterized by a normalized density $\Phi(x, t)$ (times t and position x, with $0 \leq \Phi(x, t) \leq 1$) requiring a resource M to continue its existence and competing for the same when it is scarce. We have been inspired by the Van der Waals forces and a mean field type approach to represent it. In Section 2 we propose an appropriate model for our study. In Section 3 we show results of the linear stability analysis of homogeneous solutions and pattern formation by the effect of gregarious instinct. In Section 4 we turn to a simplified model that allows analytical results and thus conceptual clarity. And finally in Section 5, we present our conclusions.

2. Model

A typical equation describing the dynamics of a population like the one from above, but with the absence of gregarious instinct and one-dimensional case is (Fisher's equation):

$$\frac{\partial \Phi}{\partial t} = (\beta M - \alpha)\Phi - \frac{\gamma}{M}\Phi^2 + D\frac{\partial^2 \Phi}{\partial x^2}. \tag{1}$$

β represents the efficiency with which the resource is used, α is a coefficient of mortality and D the diffusion coefficient. The term $-\frac{\gamma}{M}\Phi(x, t)^2$ expresses the competition between individuals by resource, and puts a ceiling on population growth. As far as M is smaller, the ceiling is lower.

To consider the gregarious instinct, we propose a potential interaction that reflects both repulsion and attraction (other forms such as a simply square repulsive plus an attractive square part produce the same qualitative effects):

$$u(r) = -\frac{u_a}{\sqrt{\pi}(r_a - u_r r_r)}\left[\exp\left(-\frac{r^2}{r_a^2}\right) - u_r \exp\left(-\frac{r^2}{r_r^2}\right)\right].$$

Here r is the distance between individuals, r_a the midrange of the gregarious instinct (agglutinating) and u_a the corresponding interaction energy, r_r the midrange of repulsive effect caused by excessive proximity and u_r the corresponding energy, but on u_a (it is considered $u_r < 1$). Factor $\frac{1}{\sqrt{\pi}(r_a - u_r r_r)}$ is introduced so that $\int_0^\infty u(r)\mathrm{d}r = 1$. Since we intend to explore situations in which $r_a \gg r_r$, we can approximate $u(r)$ as:

$$u(r) = -\frac{u_a}{\sqrt{\pi}}\frac{\exp\left(-\frac{r^2}{r_a^2}\right)}{r_a}.$$

The average effect of this interaction can be expressed with a mean field functional whose form is calculated as:

$$U_\Phi(x) = \int \mathrm{d}x' u(x' - x)\Phi(x').$$

This strategy has been used before in different contexts [12–14,10,11]. Thus, the force that is caused by $-\nabla U_\Phi(x)$, drives a current that tends to bring individuals together. Using Einstein's relationship and the fact that current can only moves to vacant sites we obtained: $J = -\Phi(1 - \Phi)\frac{D}{k_b T}\frac{\partial U_\Phi}{\partial x}$. Then, this effect is introduced to the system by adding $-\nabla.J$ to the Eq. (1), which finally can be written as:

$$\frac{\partial \Phi}{\partial t} = (\beta M - \alpha)\Phi - \frac{\gamma}{M}\Phi^2 + D\frac{\partial}{\partial x}\left[D^*\frac{\partial \Phi}{\partial x}\right] \tag{2}$$

with $D^* = 1 - \Phi(1-\Phi)\varepsilon$. Here $\varepsilon = -\frac{1}{k_bT}\frac{\partial_x U_\Phi}{\partial_x \Phi}$ measures the intensity of the gregarious instinct, is positive and generally depends on the profile $\Phi(x)$, but for the particular case of a harmonic profile $\varepsilon = \varepsilon_0 \exp(-\frac{r_a^2 k^2}{4})$, with $\varepsilon_0 = \frac{u_a}{k_bT}$ and k the wave number. We choose ε_0 as a control parameter for the gregarious instinct. As we can see, with this strategy, the gregarious instinct is incorporated as part of an effective diffusion coefficient that contributes with the opposite sign to that expected for a real process of diffusion. This not only hinders the diffusion process, but in cases where the gregarious instinct exceeds the first one, making D^* negative could fuel the construction of inhomogeneities.

The nontrivial stationary homogeneous solution (SHS) of Eq. (2) is $\omega = M(\beta M - \alpha)/\gamma$ ($\omega = 0$ is an unstable solution). If we define $\tau = \gamma/M$ and $\xi = x/L_{\text{diff}}$, where $L_{\text{diff}} = \sqrt{\frac{MD}{\gamma}}$ is a diffusion length; and also, we redefine r_a as $\frac{r_a}{L_{\text{diff}}}$ and k as kL_{diff}; then, Eq. (2) can be dimensionless:

$$\frac{\partial \Phi}{\partial \tau} = (\omega - \Phi)\Phi + \frac{\partial}{\partial \xi}\left[D^* \frac{\partial \Phi}{\partial \xi}\right]. \tag{3}$$

This is a reaction diffusion equation with special variable diffusion coefficient, since D^* can be negative for a certain region of values of the field Φ. This possibility will depend on the intensity of the gregarious instinct and does not imply a contradiction thermodynamics, since the basis for such a possibility is a agglutinating impulse caused by forces that are attractive. The shape of this diffusion coefficient is a parabola with a minimum at $\Phi = 0.5$ and whenever $\varepsilon > 4$ there is a region with $D^* < 0$. This arises out of nothing in $\Phi = 0.5$ ($\varepsilon = 4$) and widens with increasing intensity of the gregarious instinct, i.e. that region, we call the gregarious instinct domain, -GID-, when it exists, is centered at $\Phi = 0.5$. We hope that any small inhomogeneity which originates in the GID will grow and develop. We do not know if this will finally be stabilized. However, based on the results shown in Refs. [10,11], we can assume that if the stationary homogeneous solution ω falls into the GID, it will be unstable against inhomogeneous perturbation and then a pattern should be stabilized. A situation to note is that this change of variables suggests that when the resource is large, processes are slower and uniform solutions are expected (L_{diff} increases with M).

3. Instability of the homogeneous stationary solution and stable pattern

As a first assessment, we believe that if a SHS can be destabilized by a inhomogeneous linear small perturbation, then it is expected that a pattern can grow and stabilize. Due to it, we disturb the SHS with $\delta\Phi = \delta\Phi_0 \exp(\Omega_k \tau)\exp(ik\xi)$, being $\delta\Phi_0 \ll \omega$. Thus we obtained the following condition so that SHS could be destabilized by the perturbation:

$$\Omega_k = -\omega - k^2[1 - \varepsilon\omega(1-\omega)] > 0 \tag{4}$$

with $\varepsilon = \varepsilon_0 \exp(-\frac{r_a^2 k^2}{4})$. From this expression it is clear that for this option to exist, the SHS should be located in the GID.

Then, with $\Omega_k = 0$ and $\partial_k \Omega_k = 0$ we found the first mode able to destabilize the SHS:

$$k^2 = -\frac{\omega}{2} + \frac{1}{2}\sqrt{\omega(\omega + 8/r_a^2)}. \tag{5}$$

As can be observed, when the midrange of the gregarious instinct tends to infinity, the first mode able to destabilize the SHS corresponds to $k = 0$, but to the extent that r_a is restricted to a limited area to the immediate environment of the agent (like what is expected to happen), the value of the first mode able to destabilize the SHS grows as the inverse of that midrange. Replacing k^2 in condition (4) a relationship is obtained that marks the boundary of the region where a pattern could be stabilized. Fig. 1 shows this region in the plane ε_0 vs. ω, in Fig. 2 in the plane ε_0 vs. k, in Fig. 3 in the plane ε_0 vs. M, in Fig. 4 in the plane r_a/L_{diff} vs. ω and in Fig. 5 in the plane ε_0 vs. r_a/L_{diff}.

First, all the curves found confirm that there is a region of parameters where the SHS can be destabilized by a small inhomogeneous perturbation. From Fig. 1 (ε_0 vs. ω) we see that as the system is far enough from the central part of GID; the requirement that the gregarious instinct enable the destabilization of the SHS, becomes excessive. We also note that for a small midrange ($r_a \sim 0.001$) the curve tends to be symmetric about the center of the GID. ($\Phi = 0.5$), but for r_a higher ($r_a \sim 1$), this symmetry is lost. Although ε vs. M (Fig. 3) shows a similar behavior; for this curve, the symmetry is lost for r_a small, i.e. the reverse of the previous curve. On the other hand, Fig. 2 shows that when the midrange is small the unstable region moves to k largest and its size increases considerably. Fig. 4 not only shows that, as expected, the size of this region increases with the intensity of the gregarious instinct; but that it is limited by the midrange. This is consistent with the curves of Fig. 2 showing that this region tends to disappear when r_a is large enough. Finally Fig. 5 shows that a higher midrange also requires more intense gregarious instinct for the SHS and can be destabilized by an inhomogeneous perturbation. It is worth mentioning that the effective diffusion coefficient evaluated at $\Phi = w$ always holds negative on the unstable region including its boundary.

The reason why losses in the symmetry of the curves ε_0 vs. Ω for a large midrange and why it happens in reverse to the curves ε_0 vs. M has an explanation. In order to obtain such an explanation we need to resort to some approximations, one for r_a small and one for r_a large. Thus the first mode able to destabilize the SHS (see Eq. (5)) for $r_a < 0.001$ satisfies:

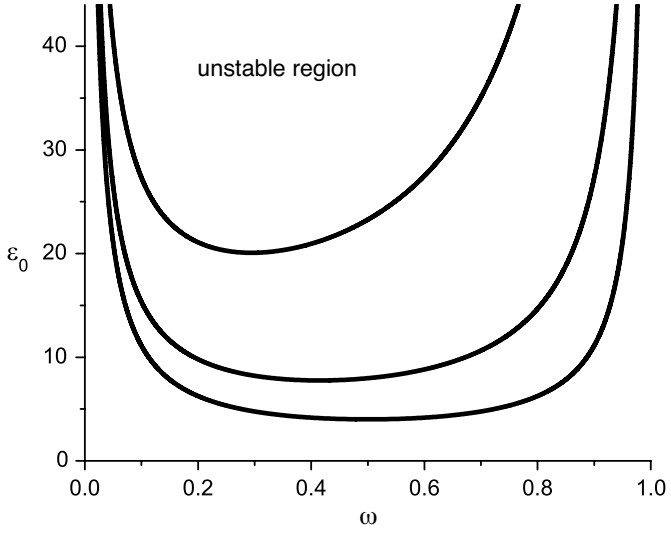

Fig. 1. Unstable region, where a pattern is likely to grow and stabilize. Gregarious instinct intensity ε_0 vs. homogeneous solution ω. Lower curve $\mapsto r_a = 0.001$, middle curve $\mapsto r_a = 1$ and upper curve $\mapsto r_a = 3$.

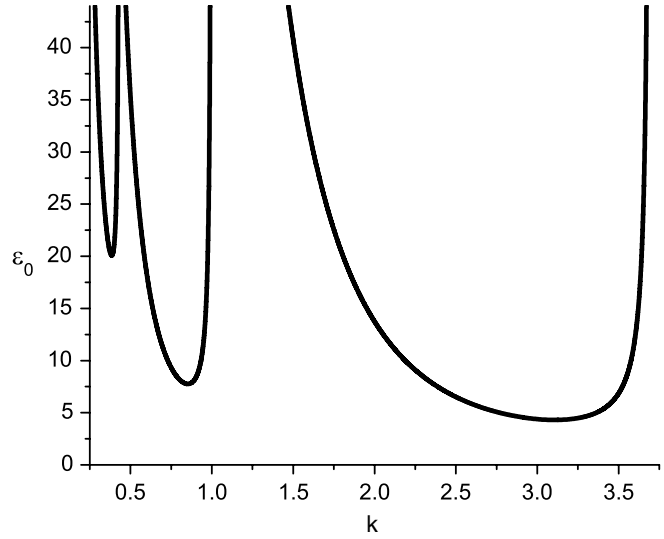

Fig. 2. Unstable region above of curves, where a pattern is likely to grow and stabilize. Gregarious instinct intensity ε_0 vs. first mode destabilizes k. Right curve $\mapsto r_a = 0.1$, middle curve $\mapsto r_a = 1$ and left curve $\mapsto r_a = 3$.

$k^2 \approx \sqrt{8\omega}/r_a$; and for $r_a > 3, k^2 \approx 4/r_a^2$. Then; replacing in Eq. (4) and by $\Omega_k = 0$ we find: $\varepsilon_0 = \frac{1}{\omega(1-\omega)}$ for the first case and, $\varepsilon_0 = \frac{1+0.25\omega r_a^2}{\omega(1-\omega)} e^1$ for the second. Both expressions fit very well with the corresponding curves in Fig. 1. The first is symmetric and the second is not. The opposite behavior of ε_0 vs. M is that ω is a quadratic form of M. When this form is replaced in calculated expressions, symmetry is restored for the second case and it is lost for the first.

To corroborate the results of our analysis we proposed cases into the unstable region and others outside of it and we solved numerically the Eq. (3) disturbing the SHS with a profile like the one used for the linear stability analysis (we proposed periodic boundary conditions). For points located in the unstable region, a pattern grew to stabilize in a profile about harmony. An example is shown in Fig. 6 [15]. While for points outside this region, the perturbation was quickly homogenized. We also tried to start the evolution from the center of the GID to points under both circumstances. Initially, it always showed a fast growth of the amplitude of the profile, regardless of whether or not SHS is linearly stable. If this is true, then an approximately harmonic pattern is stabilized. And if it is not, after such a long period of subsistence, which can become apparent stability, this pattern is rapidly homogenized. This last case occurs around the average value which varies the pattern approaching the limit of the GID and of course when a big part of the pattern has invaded the other domain (DDP), like if the pattern was attracted to that domain to be finally eliminated. Something similar was reported for a context of adsorption on surfaces with lateral interactions [10,11].

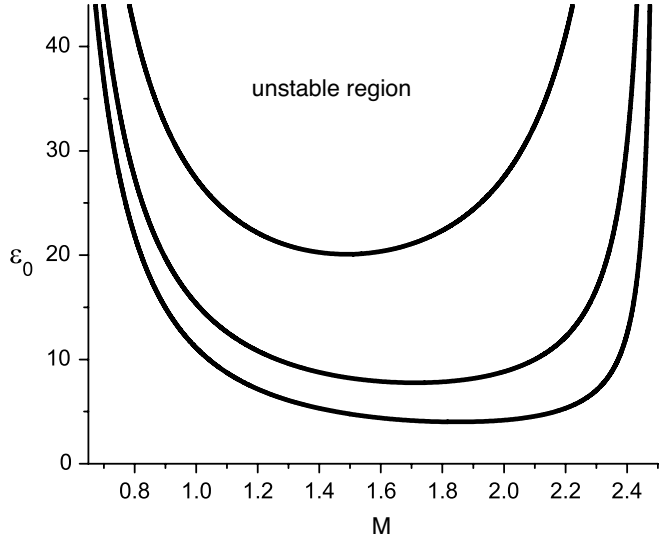

Fig. 3. Unstable region, where a pattern is likely to grow and stabilize. Gregarious instinct intensity ε_0 vs. the support M. Lower curve $\mapsto$ $r_a = 0.001$, middle curve $\mapsto$ $r_a = 1$ and upper curve $\mapsto$ $r_a = 3$.

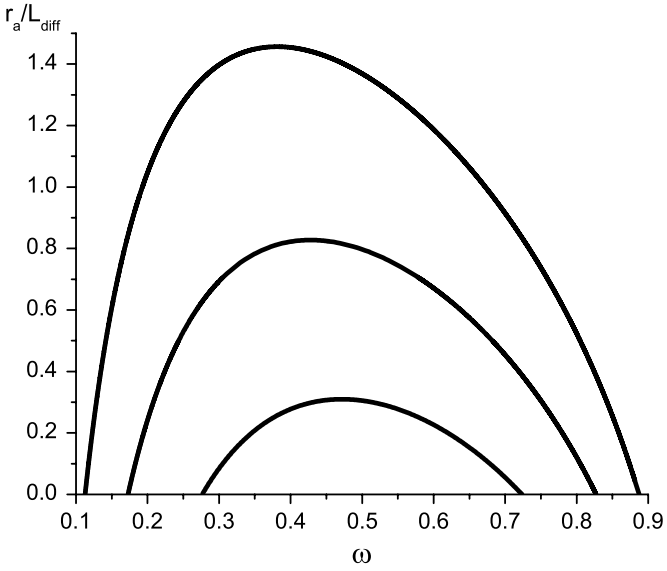

Fig. 4. Unstable region below of curves, where a pattern is likely to grow and stabilize. Mean gregarious instinct range r_a vs. homogeneous solution ω. Lower curve $\mapsto$ $\varepsilon_0 = 5$, middle curve $\mapsto$ $\varepsilon_0 = 7$ and upper curve $\mapsto$ $\varepsilon_0 = 10$.

4. Simplified model and pattern stability

Considering the fact that the inhomogeneous solutions we have found are approximately harmonic with a profile oscillating around a constant value Φ_0, and using the same idea that used in Ref. [11], we introduced in the Eq. (3):

$$\Phi(\tau, \xi) = \Phi_0(\tau) + \delta\Phi_k(\tau)\sin(k\xi).$$

Then, we consider that the main aspects that matter for the construction of the pattern are described by what happens at zero and at the ends of the profile (maximum, minimum and inflection point). Finally, after some combination of the three equations for each of these three points [11], we obtained two equations describing the evolution of $u_0(\tau) = \Phi_0(\tau) - 0.5$ and $\delta\Phi_k(\tau)$:

$$\partial_\tau \Phi_0 = Q_u, \tag{6}$$

$$\partial_\tau \delta\Phi_k = Q_r - k^2 D_p^* \delta\Phi_k. \tag{7}$$

To write these equations, we define: $Q = (\omega - \Phi)\Phi$ (see Eq. (3)) and consider that all functions with suffix $+$ are evaluated at the maximum, suffix $-$ evaluated at the minimum and suffix 0 in the zero profile; then, $Q_u = \frac{Q_+ + Q_-}{2} + Q_0$, $Q_r = \frac{Q_+ - Q_-}{2}$

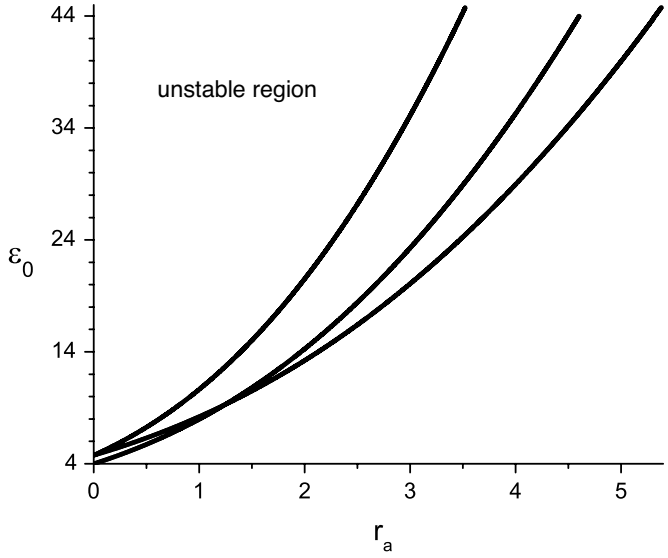

Fig. 5. Unstable region, where a pattern is likely to grow and stabilize. Gregarious instinct intensity ε_0 vs. mean gregarious instinct range r_a. Lower curve $\mapsto \omega = 0.3$, middle curve $\mapsto \omega = 0.5$ and upper curve $\mapsto \omega = 0.7$.

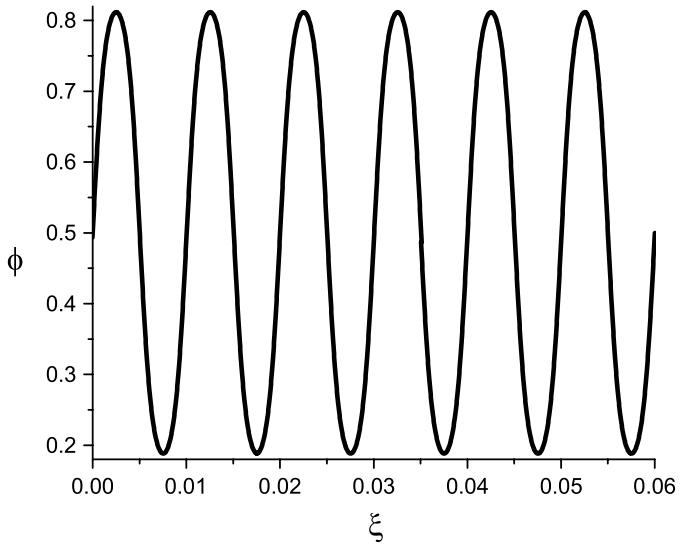

Fig. 6. Stable pattern calculated for a point in the stable region (Φ vs. ξ). $\omega = 0.5$, $\varepsilon_0 = 5$, $k = 200\pi$ and $r_a = 0.001$.

and $D_p^* = \frac{D_+^* + D_-^*}{2}$. Well,

$$Q_u = 2u_0(u_0 + 1 - \omega) + \delta\Phi_k^2 - \omega + \frac{1}{2}, \tag{8}$$

$$Q_r = -(2u_0 + 1 - \omega)\delta\Phi_k, \tag{9}$$

$$D_p^* = \varepsilon(u_0^2 + \delta\Phi_k^2 - p). \tag{10}$$

The parameter $p = \frac{\varepsilon}{4} - 1$ comes after writing the effective diffusion coefficient like $D^*(\Phi) = (\Phi - 0.5)^2 - p$, and its importance lies in the fact that this indicates the possibility of existence of a GID. If $p > 0$ there is a region of the field Φ where $D^* < 0$ and if $p < 0$ is not.

To the homogeneous solution ($\delta\Phi_k = 0$), the homogeneously stable root of $Q_u(\Phi_0) = 0$ and $Q(\Phi_0) = 0$ is the same $\Phi_0 = \omega$. Then, observing this pair of equations of evolution one expects that (6) tries to drag Φ_0 to ω and (7) in a bid to grow and then support the pattern, "tugging" of the maximum toward up and "pulling" down of minimum. If ω is located in the DDP finally the pattern is removed. Conversely, if ω is located in the GID, this will stabilize. This is verified following the evolution of equations for each case. Fig. 7 presents the case for a stabilizing pattern (the SHS is in the GID) and in Fig. 8 the case in which a pattern is not stabilized (the SHS is in the DDP). Since evolution is started from the GID, in both cases a pattern gets built, but only stabilizes that of Fig. 7. By contrast, for that whose SHS is in the DDP, when $\Phi_0(\tau)$ achieves such a domain, the pattern is quickly homogenized and the evolution of $\Phi_+(\tau)$, $\Phi_0(\tau)$ and $\Phi_-(\tau)$ overlap from that moment on.

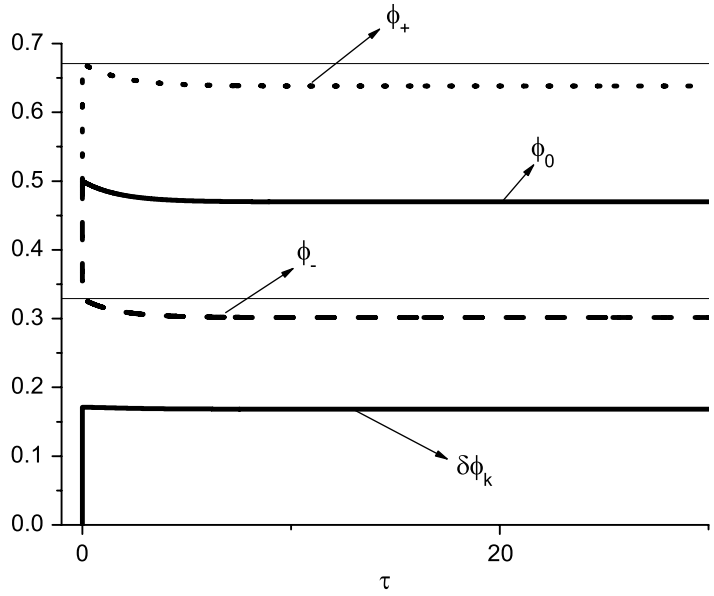

Fig. 7. Evolution of the pattern to a point of instability for stationary homogeneous solution (SHS). From top to bottom, evolution of Φ_+, Φ_0, Φ_- and $\delta\Phi_k$ for a point in the stable region. $\omega = 0.5$, $\varepsilon_0 = 5$, $k = 200\pi$ and $r_a = 0.001$. Initial condition: $\Phi_0 = 0.5$ and $\delta\Phi_k = 10^{-6}$. The GID is between the two horizontal lines and the DDP above and below them.

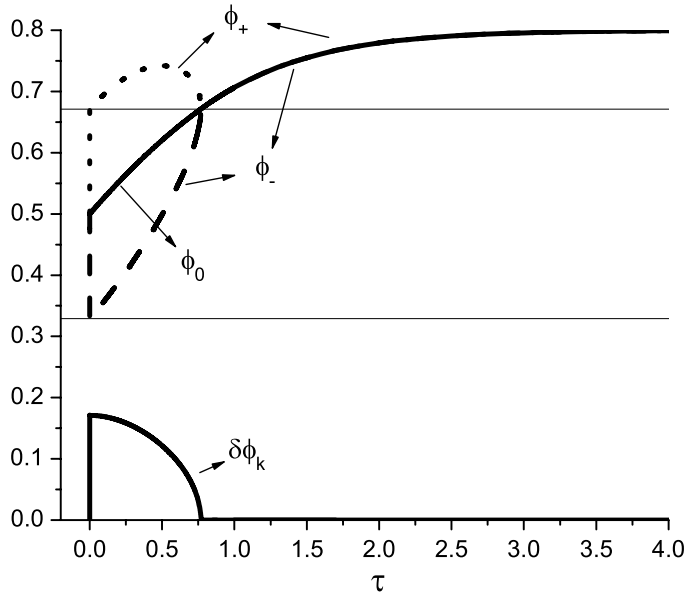

Fig. 8. Evolution of the pattern to a point of stability for stationary homogeneous solution (SHS). From top to bottom, evolution of Φ_+, Φ_0, Φ_- and $\delta\Phi_k$ for a point in the unstable region. $\omega = 0.8$, $\varepsilon_0 = 5$, $k = 200\pi$ and $r_a = 0.001$. Initial condition: $\Phi_0 = 0.5$ and $\delta\Phi_k = 10^{-6}$. The GID is between the two horizontal lines and the DDP above and below them. It is noted that $\Phi_+(\tau)$, $\Phi_0(\tau)$ and $\Phi_-(\tau)$ overlap when $\Phi_0(\tau)$ reaches the boundary between the GID and the DDP.

This behavior is the same as the one observed for the evolution calculated with Eq. (3). On the other hand, the amplitude of the pattern calculated with this equation differs from $\delta\Phi_k$ by a factor $\simeq 0.5$. Whereas in the extended case the profile is pulled from all points, while the simplified model only proposes tugging at their ends, this difference being acceptable.

With the support of these previous results we consider that this simplified model properly expresses the phenomenon described by the Eq. (3). Thus we interpret that a linear stability analysis of solutions of simplified model is also a linear stability analysis of the pattern. The stationary solutions of the Eqs. (6) and (7) can be calculated analytically and they are:

$$u_0^s = \omega - 1 + A + \sqrt{\frac{1}{4} - \omega(1-\omega) + \frac{1}{\varepsilon} + C}, \tag{11}$$

with $A = \frac{1}{k^2\varepsilon}$ and $C = \frac{1}{\varepsilon k^2}\left[3(1-\omega) + \frac{1}{\varepsilon k^2}\right]$, terms negligible when k is large enough; and

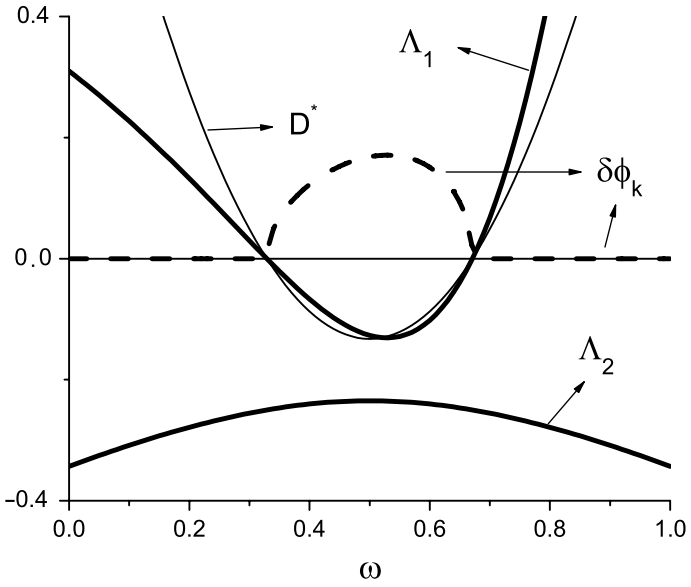

Fig. 9. Stability curves exact pattern and others. Λ_1, Λ_2, $\delta\Phi_k^s$ and D^* vs. ω. $\varepsilon_0 = 5$, $k = 200\pi$ and $r_a = 0.001$. Λ_1 and Λ_2 were rescaled to make the curves comparable on the same graph. For this value of k, overlap exact and approximate curves. $D^* < 0$ corresponds to GID and $D^* > 0$ to DDP.

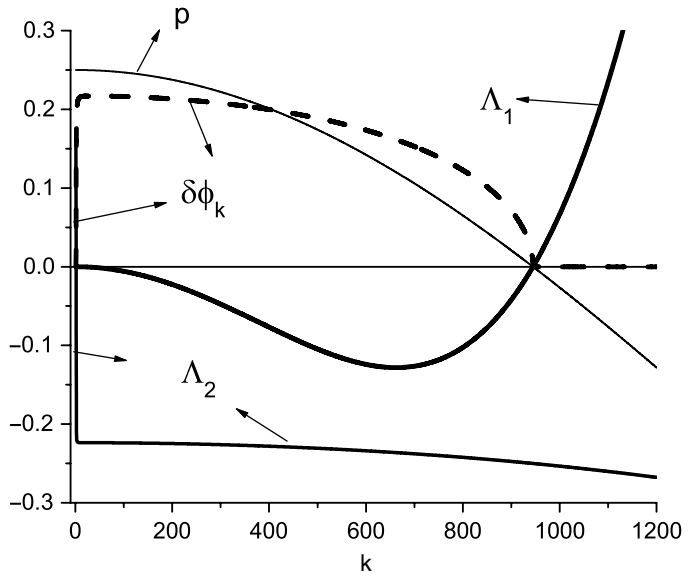

Fig. 10. Stability curves exact pattern and others. Λ_1, Λ_2, $\delta\Phi_k^s$ and p vs. k. $\varepsilon_0 = 5$, $\omega = 0.5$ and $r_a = 0.001$. Λ_1 and Λ_2 were rescaled to make the curves comparable on the same graph. For values of $k > 4$, overlap exact and approximate curves.

$$\delta\Phi_k^s = \sqrt{\omega - \frac{1}{2} - 2u_0^s(u_0^s + 1 - \omega)}. \tag{12}$$

We consider acceptable solutions to those that satisfy the condition, such that $\delta\Phi_k^s$ being real, $-1 \leq u_0^s \pm \delta\Phi_k^s \leq 1$.

Then a linear stability analysis [16] of these solutions leads to:

$$\Lambda = \frac{a+d}{2} \pm \frac{1}{2}\sqrt{(a+d)^2 - 4(ad - bc)}. \tag{13}$$

With

$$a = -2(2u_0^s + 1 - \omega), \qquad b = -2\delta\Phi_k^s$$
$$c = -2(1 + \varepsilon u_0^s k^2)\delta\Phi_k^s,$$
$$d = 2u_0^s + 1 - \omega - k^2(3\varepsilon\delta\Phi_k^{s2} + \varepsilon u_0^{s\,2} - p).$$

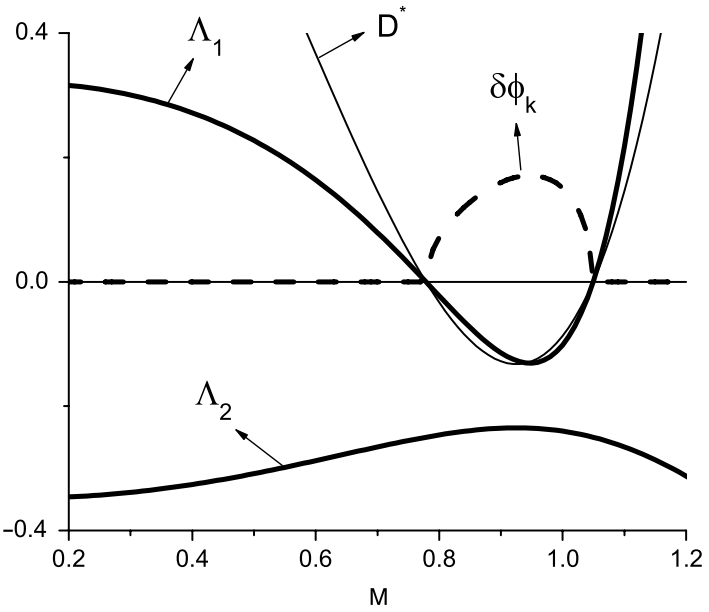

Fig. 11. Stability curves exact pattern and others. Λ_1, Λ_2, $\delta\Phi_k^s$ and D^* vs. M. $\varepsilon_0 = 5$, $k = 200\pi$ and $r_a = 0.001$. Λ_1 and Λ_2 were rescaled to make the curves comparable on the same graph. For this value of k, overlap exact and approximate curves. $D^* < 0$ corresponds to GID and $D^* > 0$ to DDP.

As we drove with the hypothesis that $k^2 \gg 1$, we found an approximate expression that fits well in the range of k that we study. Thus the stable pattern must satisfy the following two conditions:

$$\Lambda_1 = k^2 \left[p - \varepsilon (3\delta\Phi_k^{s2} + u_0^{s\,2}) \right] < 0, \tag{14}$$

$$\Lambda_2 = \omega - 1 - 2u_0^s \left(1 + \frac{\varepsilon \delta \Phi_k^{s2} k^2}{\Lambda_1} \right) < 0. \tag{15}$$

By condition (14) one might conclude that the pattern should be stable $p < 0$, however, is quite the opposite. This is made explicit if replacing u_0^s for its equivalent of Eq. (11):

$$\Lambda_1 = -k^2 \left[4p + \varepsilon B \right] < 0. \tag{16}$$

With $B = 2\omega(3 - 2\omega) - 3 + 4(1 - \omega)\sqrt{\frac{1}{4} - \omega(1 - \omega) + \frac{1}{\varepsilon}}$.

Then we plot these results as a function of the parameters that characterize the model. In Fig. 9 we show Λ_1, Λ_2, $\delta\Phi_k^s$ and D^* vs. ω. We note that the destabilization of the pattern is produced by Λ_1 when ω is within DDP. Simultaneously, $\delta\Phi_k^{s2}$ becomes negative and then $\delta\Phi_k^s$ (real part $\sqrt{\delta\Phi_k^{s2}}$) vanishes. We also note that it is higher when closer to the center of where the GID is ω located. In Fig. 10 we show Λ_1, Λ_2, $\delta\Phi_k^s$ and p vs. kL_{diff}. We note that for large k, destabilization of the pattern is due to Λ_1, while for very small k it occurs for Λ_2. Of course, this band of k changes by varying the other parameters, above all widening when ε_0 grows and shrinking when the midrange of the gregarious instinct increases. However, the main features shown in this figure are held. In Fig. 11 we show the same parameters as in Fig. 9, but varying M. So we show that when the resource is such that the effective diffusion coefficient is negative, a pattern is stabilized. Then, in Fig. 12 we observe that the parametric region where a pattern can be stabilized is limited by the midrange of the gregarious instinct. This should not exceed a maximum value, which grows with the intensity of that instinct and decreases with k. It is also noted that the amplitude of the pattern increases with ε_0. Finally, also, in Fig. 13, we plot Λ_1, Λ_2, $\delta\Phi_k^s$, Φ_0 and p vs. ε_0. Provided that $p > 0$, a pattern can be stabilized.

5. Conclusions

In this paper we characterize the gregarious instinct as the tendency of certain types of individuals (or organized structures) to join when they detect each other. We believe, as in Ref. [2], that the ability to detect each other depends on the proximity between individuals. If these individuals are too far apart they can not be detected among them. However, as in Ref. [2] we also consider that excessive proximity generates rejection. Therefore there is an intermediate range of separation between individuals where the gregarious instinct works. Then we see that this characterization can be properly described by a force like the one from Van der Waals and so defining a kind of energy of interaction between individuals we call ε_0. The measure of this parameter depends on the type of individual that it is intended to describe; but beyond this, at

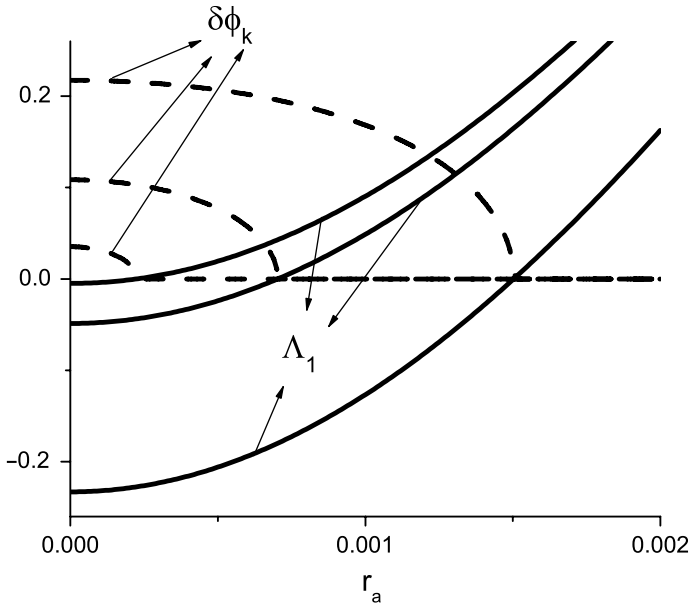

Fig. 12. Stability curves exact pattern and others. Λ_1 (solid line) and $\delta\Phi_k^s$ (dash line) vs. r_a. Λ_1 bottom–up and $\delta\Phi_k^s$ up–bottom: $\omega = 0.5$ and $\varepsilon_0 = 5$, 4.2 and 4.02. $k = 100\pi$. Λ_1 was rescaled to make the curves comparable on the same graph. For this value of k, overlap exact and approximate curves.

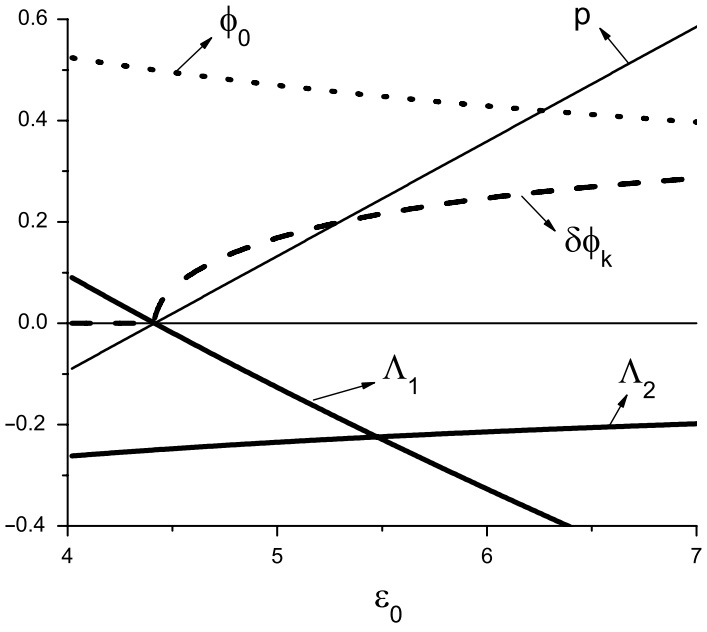

Fig. 13. Stability curves exact pattern and others. Λ_1, Λ_2, $\delta\Phi_k^s$, Φ_0 and p vs. ε_0. $\omega = 0.5$, $k = 100\pi$ and $r_a = 0.001$. Λ_1 and Λ_2 were rescaled to make the curves comparable on the same graph. For this value of k, overlap exact and approximate curves.

least, to describe the qualitative effects of gregarious instinct on this population of individuals. As mentioned in Section 2, qualitative results are independent of the model used to describe the interaction between individuals. A proof of this is that if a simple square potential instead of the form already used is proposed, the changes are minor and the qualitative results are the same. For a square interaction potential and a harmonious Fourier profile used for stability analysis of the SHS, $\varepsilon = \varepsilon_0 \frac{\sin(r_a k)}{r_a k}$, nevertheless, this does not produce qualitative changes in curve Ω_k vs. k. In Fig. 14 we show Ω_k vs. k for both proposals. You can see it is apparent that in both cases SHS is destabilized for a certain band of values of k.

Thus, we could recreate the possible consequences of this phenomenon by calculating the average effect of gregarious instinct on the population of individuals. We saw that the attractive mean field generated by the set of individuals drives them to coalesce (the opposite effect of the diffusion process). We adopt a simple system of individuals that depend on a homogeneous and continuous resource to survive, with a natural mortality rate and a term of competition for the resource that puts a cap on unlimited population growth (Fisher's equation). Then we write this model as reaction diffusion equations whose stationary solutions are homogeneous. For all these ingredients, whose result is known for a long time [8], we incorporate the gregarious instinct in the way we have said. Using a strategy already applied in another context [10,11],

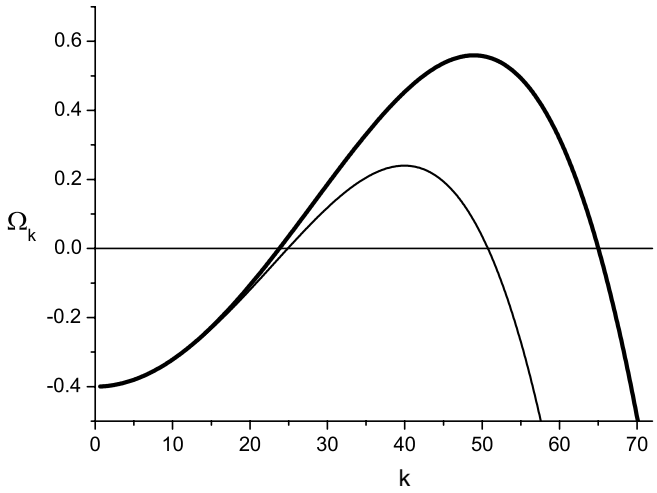

Fig. 14. Ω_k vs. k. Comparison between the two proposals for interaction, square potential (thick line) and exponential potential (fine line). $\varepsilon_0 = 4.17$, $\omega = 0.4$ and $r_a = 0.001$.

we saw that this instinct can be expressed as a negative part of an effective diffusion coefficient (D^*), that even can convert it to negative. It is clear that this coefficient should not be interpreted in the usual context of thermodynamics, since it represents two opposing phenomena. The real diffusion which tends to homogenize and the tendency to agglutinate caused by the gregarious instinct. The interesting thing about this proposal is that it could show how the gregarious instinct can lead to the construction of inhomogeneities if certain conditions are given. The main thing is that for some region of the field, D^* becomes negative. Provided that the homogeneous stationary solutions (SHS) are located in that region, which we call GID, a pattern can be stabilized. We first made a linear stability analysis of SHS and detected the region of parameters for which the SHS is unstable against inhomogeneous perturbation. We searched these regions and we found stable patterns as solutions of our system. Then, supported by this preliminary result, and inspired by a recent paper [11], we developed a simplified model that not only allowed us to reproduce the qualitative aspects of the construction and stabilization of the pattern, but also a linear stability analysis whose analytical results obtained led us to clarify the understanding of the phenomenon. We could confirm that for a pattern to stabilize the SHS actually must be located within the GID. Then, as the SHS depends on the resource, through this relationship, we showed the effect of the amount of resource on the system, whose change is likely to cause a transition from a homogeneous state to a pattern. We note that the bandwidth where it is possible that one of these patterns is stable increases with the intensity of the gregarious instinct and decreases with its midrange. Moreover, if the last is large enough, it disables the possibility of a pattern.

This work is a first step in implementing this strategy to study the possible effects of gregarious instinct in communities whose livelihoods depend on a resource that is homogeneous and constant over time and in which the effects of rule (b) are dismissed with respect to (a) and (c). One of the possible next steps is to relax these conditions.

Acknowledgments

I acknowledge financial support from CONICET, Argentina, PIP 5072/05 and UNMdP, Argentina, EXA425/08. I also acknowledge Srta. Natalia Bettiol for her great help with the English language.

References

[1] Alexander, The evolution of social behavior, Ann. Rev. Ecol. Syst. 5 (1974) 325–383;
Graeme D. Ruxton, Thomas N. Sherratt, Proc. R. Soc. B 273 (2006) 2417–2424.
[2] D.J.T. Sumpter, Phil. Trans. R. Soc. B 361 (2006) 5–22;
B.C.R. Bertram, Living in groups: predators and prey, in: J.R. Krebs, N.B. Davies (Eds.), Behavioral Ecology, first ed., Oxford: Blackwell Scientific, 1978, pp. 64–96;
D.I. Rubenstein, On Predation, Competition and the Advantages of Group Living Perspectives in Ethology 3 (1978) 205–231;
D.J. Hoare, I.D. Couzin, J.G.J. Godin, J. Kause, Animal Behaviour 67 (2004) 155–164;
D. Helbing, P. Molnár, Phys. Rev. E 51 (1995) 4282–4286.
[3] Such as bacterial populations or herds of mammals feeding on a vast field.
[4] M.A. Fuentes, M.N. Kuperman, V.M. Kenkre, Phys. Rev. Lett. 91 (2003) 158104;
E. Gilad, J. von Hardenberg, A. Provenzale, M. Shachak, E. Meron, Phys. Rev. Lett. 93 (2004) 098105;
M.G. Clerc, D. Escaff, V.M. Kenkre, Phys. Rev. E 72 (2005) 056217;
E. Hernndez-García, C. López, Phys. Rev. E 70 (2004) 016216.
[5] A. Czirók, T. Vicsek, Physica A 281 (2000) 17–29;
A. Czirók, A.L. Barabasi, T. Vicsek, Phys. Rev. Lett. 82 (1999) 209–212;
Z. Csahók, T. Vicsek, Phys. Rev. E 52 (1995) 5297.

[6] I.D. Couzin, J. Krause, R. James, G.D. Ruxton, N.R. Franks, J. Theoret. Biol. 218 (2002) 1–11;
I.D. Couzin, J. Krause, N.R. Franks, S.A. Levin, Nature 433 (2005) 513–516;
C.W. Reynolds, Comput. Graph. 21 (4) (1987) 25–34;
S. Gueron, S.A. Levin, D.I. Rubenstein, J. Theoret. Biol. 182 (1996) 85–98;
I. Farkas, D. Helbingb, T. Vicseka, Physica A 330 (2003) 18–24;
E.D. Silverman, Ecol. Model. 175 (2004) 411–424;
D. Helbing, B.A. Huberman, Nature 396 (1998) 738–740;
D. Helbing, I. Farkas, T. Vicsek, Nature 407 (2000) 487–490;
M. Zhenga, Y. Kashimoria, O. Hoshinoc, K. Fujitab, T. Kambara, J. Theoret. Biol. 235 (2005) 153–167.
[7] A. Okubo, Adv. Biophys. 22 (1986) 1–14;
S. Gueron, N.J. Liron, Math. Biol. 27 (1989) 595–608.
[8] J.D. Murray, Mathematical Biology, second ed., Springer, New York, 1993.
[9] J. von Hardenberg, E. Meron, M. Shachak, Y. Zarmi, Phys. Rev. Lett. 87 (2001) 198101;
N.M. Shnerb, P. Sarah, H. Lavee, S. Solomon, Phys. Rev. Lett. 90 (2003) 0381011;
Weiming Wang, Quan-Xing Liu, Zhen Jin, Phys. Rev. E 75 (2007) 051913;
T. Butler, N. Goldenfeld, Phys. Rev. E 80 (2009) 030902(R).
[10] S.E. Mangioni, Physica A 224 (2010) 153.
[11] S.E. Mangioni, R.R. Deza, Phys. Rev. E 82 (2010) 042101.
[12] A. Mikhailov, G. Ertl, Chem. Phys. Lett. 238 (1995) 104.
[13] M. Hildebrand, A.S. Mikhailov, G. Ertl, Phys. Rev. E 58 (11) (1998) 5483.
[14] S.B. Casal, H.S. Wio, S. Mangioni, Physica A 311 (2002) 443–457.
[15] We propose a value for the wavenumber to excite the pattern. Then the system evolves towards a stationary profile that is approximately harmonic. This does not mean that this is the only solution. The general solution will produce k contributions within the allowed bandwidth (GID) depending on which unstable modes are excited.
[16] G. Nicolis, Introduction to nonlinear science, University of Brussels.